

Image Denoising using Shiftable Directional Pyramid and Scale Mixtures of Complex Gaussians

An P.N. Vo
Department of Electrical Engineering,
University of Texas at Arlington,
Arlington, TX 76019-0016,
Email: vptonan@msp.uta.edu

Truong T. Nguyen
Geophysic Research Center,
Paris School of Mines,
Fontainebleau, 77305 France
Email: truong.nguyen@ensmp.fr

Soontorn Oraintara
Department of Electrical Engineering,
University of Texas at Arlington,
Arlington, TX 76019-0016,
Email: oraintar@uta.edu

Abstract—In this paper, a modified version of the complex directional pyramid (PDTDFB) is proposed. Unlike the previous approach, the new FB provides an approximately tight-frame decomposition. We introduced the complex Gaussian scale mixture (CGSM) for modeling the distribution of complex directional wavelet coefficients. The statistical model is then used to obtain the denoised coefficients from the noisy image decomposition by Bayes least squares estimator. Performance of the denoised images using the PDTDFB is compared to the conventional transforms including the orthogonal wavelet, the contourlet and the steerable pyramid. The experiments show that the PDTDFB could achieve higher quality image denoising than the wavelet and the contourlet with the hard thresholding method, and is comparable to the steerable pyramid in terms of mean squared error (MSE) and perceptual image quality (SSIM) with the Bayes least squares estimator.

I. INTRODUCTION

Many applications in image processing such as image compression, image denoising can benefit from a statistical model to characterize the image in the transform domain. A clean, precise probability model which can describe sufficiently typical images becomes essential. In this paper, the complex Gaussian scale mixture model for the shiftable complex directional pyramid decomposition (PDTDFB [1]) is proposed for image denoising through the Bayes least squares estimator.

There are many works on the statistics of decomposition coefficients of the wavelet transform [2]. The wavelet coefficients within a subband were often assumed to be independent and identically distributed. With this assumption, the wavelet coefficients can be modeled by the marginal model whose distribution is a two-parameter generalized Gaussian density (GGD). The GGD is very suitable distribution for the peaky and heavy-tailed non-Gaussian statistic of typical image wavelet decomposition. Although this wavelet marginal model is more powerful than the Gaussian model, it does not take into account the dependencies between different subbands as well as between a coefficient and its neighboring coefficients of the same subband. A number of researchers have developed successfully joint statistical models in wavelet domain [3][4][5]. The Hidden Markov Tree was introduced in [3] to model the wavelet decomposition. A bivariate probability density function has been proposed to model the statistical dependencies between a wavelet coefficient and its parent [5]. In [4], the author developed a model for neighborhoods of oriented pyramid coefficients based on a Gaussian scale mixture (GSM) which is the product of a Gaussian random vector and an independent hidden random scalar multiplier. This model can account for both marginal and pairwise joint distributions of wavelet coefficients. The GSM estimator is more complex than Gaussian or wavelet marginal estimators but it provides significantly higher performances in terms of both mean square error and visual quality in image denoising [6].

In image analysis applications, an overcomplete, multiresolution and multidirectional representation usually provides much better performance compared to the critical representation such as the discrete wavelet transform (DWT). Examples of multiscale and multidirectional decompositions include Gabor filter bank, steerable pyramid [7], complex wavelet, contourlet transform [8] and the PDTDFB decomposition [1].

In this paper, we develop image denoising algorithm in PDTDFB domain based on the complex Gaussian scale mixture (CGSM). The pyramid FB in the PDTDFB is modified using other pyramidal structure than the Laplacian pyramid. If there is added noise in the decomposition coefficients of an image, the noise will be minimized in the reconstruction image thanks to the new pyramid structure. The paper is organized as follows. In the next section, the modified shiftable complex directional pyramid is presented. The CGSM distribution of local neighborhoods around a complex coefficient is defined in Section III. We present the algorithm and experiments for image denoising in Section IV. Section V concludes the paper.

II. THE MODIFIED SHIFTABLE COMPLEX DIRECTIONAL PYRAMID

The shiftable complex directional pyramid is a new image decomposition, which is recently proposed in [1]. The image decomposition implemented by a filter bank (FB) consists of a Laplacian pyramid and a pair of directional filter banks (DFBs), designated as primal and dual DFBs. Both DFBs are constructed by a binary-tree of two-channel fan FBs. The filters of these FBs are designed to have special phase functions so that the overall directional filters of the dual DFB are the Hilbert transforms of the corresponding filters in the primal DFB. Therefore, the two DFBs can be viewed as a single FB with complex directional filters producing complex subband images, whose real and imaginary parts are the outputs of the primal and dual DFB, respectively. A multiresolution representation is obtained by reiterating the decomposition at the lowpass branch. It is shown in [1] that if the lowpass filters used in the Laplacian pyramid have bandpass regions restricted in $[-\pi/2, \pi/2]^2$, then the complex directional subbands at all scale are shiftable.

The object of combining the Laplacian pyramid and dual-tree DFB is to provide a FB that is multiresolution and multidirectional at the same time. However, the Laplacian pyramid structure is not essential to the shiftability of the overall FB. In fact, we can combine any shiftable two-channel 2-D multiresolution FB with the dual-tree DFB to obtain an overall shiftable FB. Moreover, it can be shown that the synthesis side of the Laplacian pyramid structure is suboptimal. In this paper, we proposed the construction of a shiftable FB by combining the dual-tree DFBs with a multiresolution FB as in Fig 1. The advantage of the new FB is that it provides an approximately tight-frame decomposition, which is a desirable

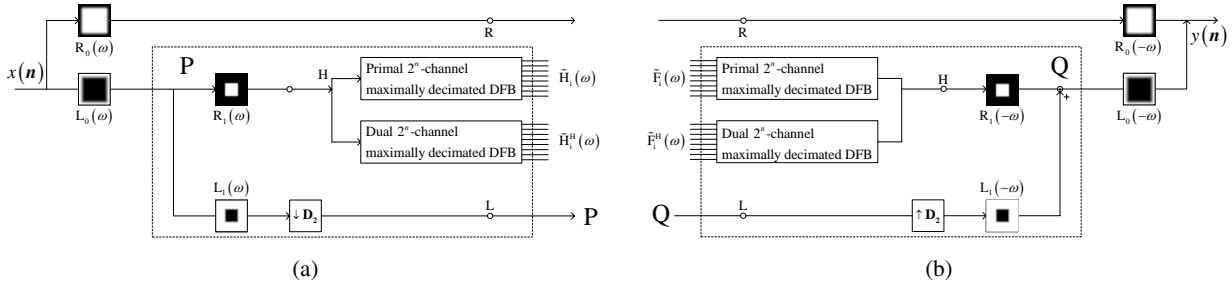


Fig. 1. A shiftable pyramid [1]. (a) The analysis side, and (b) Synthesis side. Similar P and Q blocks can be reiterated at lower scale to decompose an image into a multiscale representation.

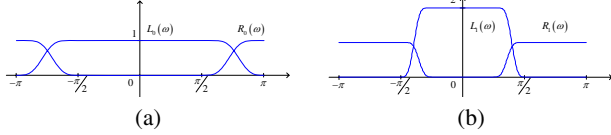


Fig. 2. A slice of the 2-D frequency responses of (a) $R_0(\mathbf{z})$ and $L_0(\mathbf{z})$, (b) $R_1(\mathbf{z})$ and $L_1(\mathbf{z})$.

property in an overcomplete decomposition [2]. However, the FB is no longer exactly perfect reconstruction and the pyramidal filters are nonseparable.

The new structure for the PDTDFB is illustrated in Fig. 1. The input image is first pass through a two-channel undecimated FB. The filters satisfy perfect reconstruction (PR) condition:

$$|R_0(\omega)|^2 + |L_0(\omega)|^2 = 1. \quad (1)$$

The filter $L_0(\mathbf{z})$ is a wide-band lowpass filter while $R_0(\mathbf{z})$ is a highpass filter. A slice of the two-dimensional frequency responses of these two filters are in Fig. 2(a). After the undecimated FB, the PDTDFB consists of multiple levels of block P (or Q for the synthesis side) for each scale. This block consists of two filters $R_1(\mathbf{z})$ and $L_1(\mathbf{z})$ and the dual-tree DFBs. The low frequency component, after filtered by the low-pass filter $L_1(\mathbf{z})$ and decimated by $\mathbf{D}_2 = 2\mathbf{I}$, is fed into the second level decomposition for the second resolution of directional subbands. The filters in blocks P and Q are designed to satisfy the PR and non-aliasing condition (see Fig. 2(b))

$$|R_1(\omega)|^2 + \frac{1}{4}|L_1(\omega)|^2 = 1, \quad (2)$$

$$L_1(\omega_1, \omega_2) = 0 \text{ when } |\omega_1| > \frac{\pi}{2} \text{ or } |\omega_2| > \frac{\pi}{2}. \quad (3)$$

The above conditions can only be approximated by realizable filters. Similar to the steerable pyramid [7], the analysis filters are the inverse of the synthesis filters. The implementation of the pyramid FB is in the Fourier domain. The filters $R_i(\mathbf{z})$ and $L_i(\mathbf{z})$ are defined based on the 1-D Meyer scaling function [2].

III. SCALE MIXTURE OF COMPLEX GAUSSIAN DISTRIBUTIONS

A. Complex Gaussian distributions

A complex Gaussian distribution is defined as follows [9][10]:

$$f(\mathbf{u}) = \frac{\exp(-\mathbf{u}^H (\mathbf{C}_u)^{-1} \mathbf{u})}{(\pi)^N |\mathbf{C}_u|}, \quad (4)$$

where $\mathbf{u} \in \mathbf{C}^{N \times 1}$ is a vector of complex stochastic variable defined as $\mathbf{u} = (u_1, u_2, \dots, u_N)^T$, and $u_n = x_n + jy_n$, $x_n, y_n \in \mathbf{R}^1$, real-valued variables normally distributed. It will be assumed that

$E[u_n] = E[x_n] + jE[y_n] = 0$, where $E[\cdot]$ is expectation operator. In these expressions, the superscript T denotes transposition, the superscript H denotes complex conjugate transposition, and $j = \sqrt{-1}$. Furthermore, $\mathbf{C}_u \in \mathbf{C}^{N \times N}$ is the complex covariance matrix defined as $\mathbf{C}_u = E[\mathbf{u}\mathbf{u}^H]$. By definition, \mathbf{C}_u is positive definite and Hermitian symmetric, hence, its inverse exists.

B. Complex Gaussian scale mixture for complex coefficient model

A statistic model based on Gaussian scale mixture distribution, which is the product of a Gaussian random vector and an independent hidden random scalar multiplier, is developed in [4]. This model can account for both marginal and pairwise joint distributions of real wavelet coefficients. Inspired by this approach, we define a complex Gaussian scale mixture for modeling the complex coefficients. If two random variables (x, z) have a jointly distribution, a mixture of $f(x)$ distributions is defined [11] as follows

$$h(x) = \int f(x|z)g(z)dz, \quad (5)$$

where $f(x)$ and $g(z)$ are the probability density functions of x, z .

Suppose that the vector \mathbf{u} has a complex Gaussian distribution and that scalar real variable \sqrt{z} has some distribution on $(0, \infty)$ with a density $p_z(z)$ ($z > 0$). We refer $\mathbf{x} \triangleq \sqrt{z}\mathbf{u}$ as the scale mixtures of complex Gaussian distribution as follows

$$p_{\mathbf{x}}(\mathbf{x}) = \int p(\mathbf{x}|z)p_z(z)dz, \quad (6)$$

$$p_{\mathbf{x}}(\mathbf{x}) = \int \frac{\exp(-\mathbf{x}^H (z\mathbf{C}_u)^{-1} \mathbf{x})}{(\pi)^N |z\mathbf{C}_u|} p_z(z)dz, \quad (7)$$

where $\mathbf{C}_u = E[\mathbf{u}\mathbf{u}^H]$ is complex covariance matrix of \mathbf{u} , $\mathbf{u} = (u_1, u_2, \dots, u_N)^T$, and N is dimensionality of \mathbf{u} and \mathbf{x} . The density of \mathbf{x} is complex Gaussian when conditioned on z , and the variable z is known as the multiplier. We assume that the coefficients $\mathbf{x} = \mathbf{x}_{real} + j\mathbf{x}_{imag}$ within each local neighborhood around a reference coefficient of a complex subband are characterized by a CGSM model. In general, the neighborhood may include coefficients from other subbands, as well as from the same subbands. Similar to the GSM, the probability density of the multiplier $p_z(z)$ can be founded by using maximum log likelihood approach for estimating a nonparametric $p_z(z)$ from an observed set of M neighborhood vectors.

$$\hat{p}_z(z) = \arg \max_{p_z(z)} \sum_{m=1}^M \log \int_0^\infty p(\mathbf{x}_m|z)p_z(z)dz. \quad (8)$$

The PDTDFB coefficients are linked indirectly by their shared dependency on the hidden multipliers z . Hence, the CGSM model

can describe the shape of complex wavelet coefficient distributions and the correlation between neighbor coefficients. Furthermore, the CGSM model captures both magnitude and phase information of the natural image.

IV. IMAGE DENOISING APPLICATION

A. Thresholding

1) *Experiments:* In the first set of experiments, the images are denoised by using the hard thresholding method. We decompose images into subbands using the PDTDFB, DWT and contourlet FBs. All the three decompositions have four resolution levels, and the lowest resolution subbands (coarse signal) are kept unchanged. An orthogonal and nearly linear phase *symlet* FB of length 10 is used in the DWT decomposition. In the contourlet and PDTDFB decomposition, the two lower resolution levels are also *symlet* wavelet, while the two higher levels are directional FBs with 32 subbands and 16 subbands at the highest resolution and the next lower resolution, respectively. The added noise is Gaussian and white with variance σ^2 . The threshold is set at three times of the standard deviation of the noise in the subbands. The noise variance in the wavelet subband is also σ^2 , since the wavelet is orthonormal. The noise variances in the directional subbands of the PDTDFB decomposition are estimated by

$$\begin{aligned}\sigma_k^2 &= \frac{1}{4\pi^2} \int \sigma^2 |F_k(\omega)|^2 d\omega \\ &= \sigma^2 \sum_{\mathbf{n} \in \mathbb{Z}^2} |f_k(\mathbf{n})|^2\end{aligned}\quad (9)$$

where $f_k(\mathbf{n})$ and $F_k(\omega)$ are the spatial and frequency responses of the k^{th} considered directional filter.

2) *Results:* We compare the PSNR values of the denoising results using different transforms with the hard thresholding method as shown in table I. The PDTDFB transform provides higher PSNR values than the wavelet and contourlet transforms for three images. It is evident that the PDTDFB is consistently better than the wavelet and contourlet transforms when the standard deviation of the input noise is varying between $\sigma = 15$ and $\sigma = 100$.

B. Bayes Least Squares Estimator

One of the best methods for image denoising is the Bayes least squares estimator based on the Gaussian scale mixture model (BLS-GSM) presented in [6]. For each neighborhood, the reference coefficient at center of the neighborhood is estimated from \mathbf{y} , the set of observed coefficients. The subband coefficients are real numbers, and the probability density function is a function of the real variable. The BLS-GSM method is used to estimate the real subband coefficients. However, the shiftable complex directional pyramid decomposes an image into the subbands whose coefficients are complex values. Our purpose here is to develop the BLS-GSM algorithm for estimating the complex coefficients.

Let \mathbf{y} be the vector corresponding to a neighborhood of N observed complex coefficients

$$\mathbf{y} = \mathbf{x} + \mathbf{w}, \quad (10)$$

where \mathbf{x} is a original coefficient vector and \mathbf{w} is a noise vector in the transform domain. We make a simplifying assumption that \mathbf{w} is a zero-mean complex Gaussian vector and \mathbf{x} is a CGSM vector as shown in (7). It is well know that the Bayes least squares estimation is the conditional expectation when \mathbf{x} and \mathbf{y} are real random vectors as follows

$$\hat{\mathbf{x}} = E[\mathbf{x}|\mathbf{y}]. \quad (11)$$

TABLE I
PSNR VALUES OF THE IMAGE DENOISING EXPERIMENTS USING HARD THRESHOLDING METHOD

| Image | σ | PSNR | DWT | contourlet | PDTDFB |
|---------|----------|-------|-------|------------|--------------|
| Lena | 15 | 24.61 | 30.03 | 30.32 | 31.98 |
| | 20 | 22.11 | 28.67 | 29.11 | 30.83 |
| | 30 | 20.17 | 26.67 | 27.41 | 28.95 |
| | 50 | 14.15 | 24.05 | 25.10 | 26.39 |
| | 75 | 10.63 | 21.73 | 23.12 | 24.04 |
| | 100 | 8.13 | 19.84 | 21.68 | 22.33 |
| Barbara | 15 | 24.61 | 27.31 | 27.59 | 29.32 |
| | 20 | 22.11 | 25.70 | 26.38 | 28.06 |
| | 30 | 20.17 | 23.62 | 24.68 | 26.52 |
| | 50 | 14.15 | 21.52 | 22.70 | 24.31 |
| | 75 | 10.63 | 19.86 | 21.13 | 22.45 |
| | 100 | 8.13 | 18.31 | 19.99 | 20.99 |
| Peppers | 15 | 24.61 | 29.87 | 29.95 | 31.09 |
| | 20 | 22.11 | 28.51 | 28.92 | 30.00 |
| | 30 | 20.17 | 26.52 | 27.17 | 28.46 |
| | 50 | 14.15 | 23.87 | 24.94 | 26.10 |
| | 75 | 10.63 | 21.56 | 23.05 | 23.83 |
| | 100 | 8.13 | 19.58 | 21.47 | 22.18 |

$$E[\mathbf{x}|\mathbf{y}] = \int_0^\infty p(z|\mathbf{y})E[\mathbf{x}|\mathbf{y}, z]dz, \quad (12)$$

where the scalar real variable z has some distribution on $(0, \infty)$ with a density $p_z(z)$ ($z > 0$). When conditioned on z as shown in [6]

$$E[\mathbf{x}|\mathbf{y}, z] = z\mathbf{C}_u(z\mathbf{C}_u + \mathbf{C}_w)^{-1}\mathbf{y}. \quad (13)$$

It is possible to show that the same results (11), (12), (13) are valid for the complex random variables. However, the covariance matrices $\mathbf{C}_u = E[\mathbf{u}\mathbf{u}^H]$ and $\mathbf{C}_w = E[\mathbf{w}\mathbf{w}^H]$ are positive definite and Hermitian symmetric ($c_{i,j} = c_{j,i}^*$), and the density of the observed neighborhood vector conditioned on z is a zero-mean complex Gaussian, with covariance $\mathbf{C}_y|_z = z\mathbf{C}_u + \mathbf{C}_w$

$$p(\mathbf{y}|z) = \frac{\exp(-\mathbf{y}^H(z\mathbf{C}_u + \mathbf{C}_w)^{-1}\mathbf{y})}{(\pi)^N |z\mathbf{C}_u + \mathbf{C}_w|}, \quad (14)$$

For estimating \mathbf{x} , $p(z|\mathbf{y})$ as in (12) is computed as follows

$$p(z|\mathbf{y}) = \frac{p(\mathbf{y}|z)p_z(z)}{\int_0^\infty p(\mathbf{y}|\alpha)p_z(\alpha)d\alpha}, \quad (15)$$

and $p_z(z) \propto 1/z$ as shown in [6] is applied to the experiments in this paper.

1) *Experiments:* We decompose the images into subbands using a shiftable complex directional pyramid [1]. The representation consists of oriented bandpass bands at 3 scales (16 orientations in the finest scale, 8 orientations in the coarse scale and 4 orientations in the coarsest scale), highpass residual band, and one lowpass band. Each subband except for the lowpass residual band is denoised by using the BLS estimator described above. The denoised image is reconstructed from the processed subbands and the lowpass band. We assume the image is corrupted by independent additive Gaussian noise. The Lena, Barbara images of size 512×512 are used in this experiment.

We obtain the neighborhood noise covariance \mathbf{C}_w by decomposing a random noise image which has normal distribution with mean zero, standard deviation σ and dimensionality as original image in to shiftable complex pyramid subbands. This image has the same power spectrum as the noise. Given \mathbf{C}_w , the covariance \mathbf{C}_u can be computed from the observation covariance matrix $\mathbf{C}_y = E[z]\mathbf{C}_u + \mathbf{C}_w$. Set $E[z] = 1$, hence, $\mathbf{C}_u = \mathbf{C}_y - \mathbf{C}_w$.

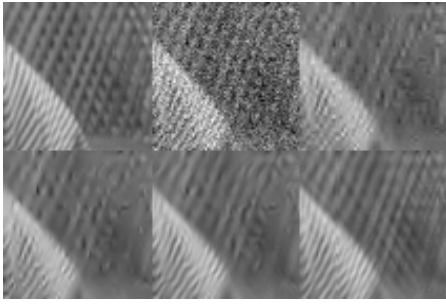


Fig. 3. Comparison of denoising results on Barbara. From left to right and top to bottom: Original image, Noisy image ($\sigma = 25$, $PSNR = 20.17$), DWT ($PSNR = 27.05$), UDWT ($PSNR = 28.06$), FS ($PSNR = 29.13$), and PDTDFB ($PSNR = 29.38$).

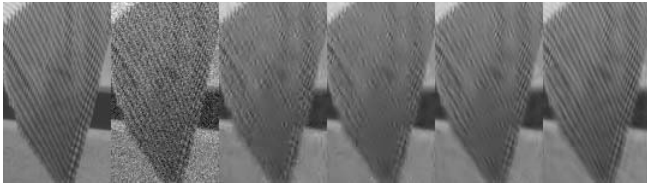


Fig. 4. Comparison of denoising results on Barbara. From left to right: Original image, Noisy image ($\sigma = 25$, $PSNR = 20.17$), DWT ($PSNR = 27.05$), UDWT ($PSNR = 28.06$), FS ($PSNR = 29.13$), and PDTDFB ($PSNR = 29.38$).

2) *Results:* Table II and III show the PSNR and SSIM [12] values of the denoising results when the standard deviation of the input noise is varying between $\sigma = 15$ and $\sigma = 100$. The quality of the denoised images of our proposed denoising method are compared to those of BLS-GSM method [6] in wavelet domain including orthogonal wavelet (DWT) and full steerable pyramid (FS). Our method performs better than the orthogonal wavelet in terms of mean squared error (MSE) and perceptual image quality (SSIM) and is comparable to the steerable pyramid with several noise levels σ from 15 to 100. This is significant since the PDTDFB has much lower overcomplete ratio compared to the steerable pyramid. The PDTDFB redundancy ratio approximately 11/3, while the redundancy ratio of the steerable pyramid with 8 orientations is 32/3. The proposed denoising method could achieve high quality image denoising, recover very fine details, e.g. texture. Figure 3 and 4 show the zoom-in image denoising results of Barbara image with different denoising methods. In these figures, UDWT denotes the undecimated discrete wavelet transform.

V. CONCLUSION

The modified version of the PDTDFB has been proposed for image denoising. The shiftable properties of this approximately tight-frame decomposition benefits the image denoising application. In comparison to the existing transforms including the wavelet, the contourlet, the PDTDFB yields the best image denoising performance with the thresholding method. Although the overcomplete ratio of the PDTDFB is much lower than this of steerable pyramid, by combining the CGSM model with BLS estimator, PDTDFB could achieve the denoised image quality comparable to steerable pyramid with the BLS-GSM algorithm.

VI. ACKNOWLEDGMENT

This work was supported in part by NSF Grant ECS-0528964.

TABLE II
PSNR VALUES OF THE IMAGE DENOISING EXPERIMENTS USING BAYES
LEAST SQUARES ESTIMATOR

| Image | σ | PSNR | FS [6] | DWT | PDTDFB |
|---------|----------|-------|--------------|-------|--------------|
| Lena | 15 | 24.61 | 33.90 | 32.39 | 33.56 |
| | 20 | 22.11 | 32.66 | 31.04 | 32.31 |
| | 25 | 20.17 | 31.69 | 30.01 | 31.33 |
| | 50 | 14.15 | 28.61 | 27.01 | 28.04 |
| | 75 | 10.63 | 26.84 | 24.41 | 26.06 |
| | 100 | 8.13 | 25.64 | 23.21 | 24.60 |
| Barbara | 15 | 24.61 | 31.86 | 29.88 | 31.86 |
| | 20 | 22.11 | 30.32 | 28.24 | 30.45 |
| | 25 | 20.17 | 29.13 | 27.05 | 29.38 |
| | 50 | 14.15 | 25.48 | 23.82 | 26.04 |
| | 75 | 10.63 | 23.65 | 22.32 | 24.16 |
| | 100 | 8.13 | 22.61 | 21.44 | 22.73 |

TABLE III
SSIM VALUES OF THE IMAGE DENOISING EXPERIMENTS USING BAYES
LEAST SQUARES ESTIMATOR

| Image | σ | SSIM | FS | DWT | PDTDFB |
|---------|----------|------|-------------|------|-------------|
| Lena | 15 | 0.45 | 0.89 | 0.86 | 0.88 |
| | 20 | 0.34 | 0.87 | 0.83 | 0.86 |
| | 25 | 0.27 | 0.85 | 0.80 | 0.84 |
| | 50 | 0.11 | 0.78 | 0.69 | 0.77 |
| | 75 | 0.06 | 0.73 | 0.59 | 0.71 |
| | 100 | 0.04 | 0.69 | 0.53 | 0.65 |
| Barbara | 15 | 0.58 | 0.90 | 0.86 | 0.90 |
| | 20 | 0.48 | 0.87 | 0.82 | 0.87 |
| | 25 | 0.40 | 0.84 | 0.78 | 0.85 |
| | 50 | 0.20 | 0.70 | 0.62 | 0.73 |
| | 75 | 0.11 | 0.61 | 0.53 | 0.65 |
| | 100 | 0.07 | 0.53 | 0.47 | 0.58 |

REFERENCES

- [1] T. Nguyen and S. Orintara, "The shiftable complex directional pyramid," *submitted to IEEE Transactions on Image Processing*, 2006. [Online]. Available: <http://www-ee.uta.edu/msp/truong>
- [2] S. G. Mallat, *A wavelet tour of signal processing*. San Diego: Academic Press, 1998.
- [3] M. Course, R. D. Nowak, and R. G. Baraniuk, "Wavelet-based signal processing using hidden Markov models," *IEEE Trans. Signal Processing*, (Special Issue on Wavelet and Filter banks), pp. 886–902, Apr 1998.
- [4] M. J. Wainwright and E. P. Simoncelli, "Scale mixtures of Gaussians and the statistics of natural images," *Adv. Neural Information Processing Systems*, vol. 12, pp. 855–861, 2000.
- [5] L. Sendur and I. Selesnick, "Bivariate shrinkage functions for wavelet-based denoising exploiting interscale dependency," *IEEE Transactions on Signal Processing*, vol. 50, no. 11, Nov 2002.
- [6] J. Portilla, V. Strela, M. J. Wainwright, and E. P. Simoncelli, "Image denoising using scale mixtures of Gaussians in the wavelet domain," *IEEE Trans. Image Processing*, vol. 12, no. 11, Nov 2003.
- [7] E. P. Simoncelli, W. T. Freeman, E. H. Adelson, and D. J. Heeger, "Shiftable multiscale transform," *IEEE Transaction on Information Theory*, vol. 38, no. 2, pp. 587–607, Mar 1992.
- [8] M. N. Do and M. Vetterli, "The contourlet transform: An efficient directional multiresolution image representation," *IEEE Transactions on Image Processing*, p. in press, 2005.
- [9] N. Woodman, "Statistical analysis based on a certain multivariate complex Gaussian distribution," *Annals Math. Statist.*, vol. 34, 1963.
- [10] K. Miller, "Complex Gaussian processes," *SIAM Rev.*, vol. 11, 1969.
- [11] H. Woodman, "On the mixture of distributions," *Annals Math. Statist.*, vol. 31, no. 1, March 1960.
- [12] Z. Wang, A. Bovik, H. Sheikh, and E. Simoncelli, "Image quality assessment: from error visibility to structural similarity," *IEEE Transactions on Image Processing*, vol. 13, no. 4, April 2004.